Enzyme Models

DOI: 10.1002/ange.200603486

A Structural and Functional Model for Dioxygenases with a 2-His-1-carboxylate Triad**

*Paul D. Oldenburg, Chun-Yen Ke, A. Alex Tipton, Albert A. Shteinman, and Lawrence Que, Jr.**

Nature has evolved many oxygen-activating enzymes that catalyze a variety of metabolically important oxidations.[1] In the subset containing mononuclear non-heme iron active sites, the 2-His-1-carboxylate facial triad has emerged as a common coordinative motif in which two His residues and either an Asp or Glu residue occupy one face of the iron octahedron.[2] The remaining coordination sites can then be utilized for binding and activating the substrate and/or O_2. Although the available crystallographic data for enzymes with this motif shows the carboxylate ligand to be monodentate in most cases, bidentate carboxylate binding has been demonstrated for naphthalene dioxygenase (NDO)[3] and nitrobenzene dioxygenase (NBDO)[4] in their substrate-bound forms. NDO and NBDO are classified as Rieske dioxygenases, enzymes that initiate the biodegradation of aromatic molecules in soil bacteria by carrying out a novel *cis*-dihydroxylation of the aromatic ring.[5] Based on crystallographic data of their ESO_2 adducts, O_2 activation is thought to proceed through a side-on bound dioxygen moiety that delivers two oxygen atoms stereospecifically to the aromatic substrate.[3,5c] Thus, two *cis*-oriented labile sites on the iron center are important for dioxygen activation.

The recent emergence of the 2-His-1-carboxylate facial triad as a recurring motif for many non-heme iron enzymes[2d] has spurred efforts to obtain synthetic models for this class of enzymes. Some success has been achieved in obtaining structural models by using N,N,O ligand sets (Scheme 1);[6] however, only one of these, **3**, serves as a functional model and its O ligand is not a carboxylate, but an amide carbonyl

[*] P. D. Oldenburg, Dr. C.-Y. Ke, Dr. A. A. Tipton, Prof. Dr. L. Que, Jr.
Department of Chemisty and Center for Metals in Biocatalysis
University of Minnesota
207 Pleasant Street SE, Minneapolis, MN 55455 (USA)
Fax: (+1) 612-624-7029
E-mail: que@chem.umn.edu
Prof. Dr. A. A. Shteinman
Institute of Problems of Chemical Physics
Russian Academy of Sciences
Chernogolovka, Moscow Region 142432 (Russia)

[**] This work was supported by the U.S. Department of Energy (DOE DE-FG02-03ER15455) and the U.S. Civilian Research and Development Foundation (CRDF RC1-2058). We would like to acknowledge Dr. Maren Pink and Dr. Victor G. Young, Jr. and the X-Ray Crystallographic Laboratory of the University of Minnesota for solving the structure of complex **1**-Cl.

Supporting information (including characterization data) for this article is available on the WWW under http://www.angewandte.org or from the author.

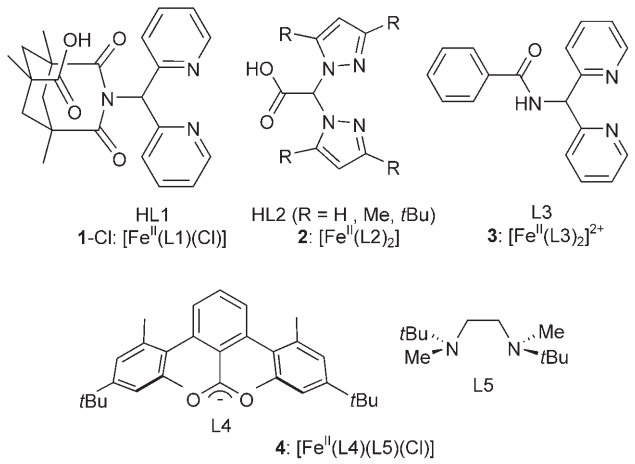

Scheme 1. The structures of HL1 and other ligands used to model 2-His-1-carboxylate non-heme iron enzymes (see Ref. [6]).

instead.[6c] Herein, we report the synthesis of a new polydentate ligand HL1 (Scheme 1) that provides two pyridines and one bidentate carboxylate. Iron(II) complexes of this ligand activate H_2O_2 to carry out olefin epoxidation and *cis*-dihydroxylation, thereby serving as both structural and functional models for the active site of the Rieske dioxygenases.

The ligand 3-(dipyridin-2-yl-methyl)-1,5,7-trimethyl-2,4-dioxo-3-azabicyclo[3.3.1]nonane-7-carboxylic acid (HL1, Scheme 1) was synthesized from the reaction of Kemp's acid chloroanhydride[7] with di(2-pyridyl)methylamine[8] by using 4-dimethylaminopyridine (DMAP) as a catalyst. Combination of deprotonated HL1 and $Fe^{II}Cl_2$ in CH_3CN afforded the complex $[Fe^{II}(L1)Cl]$ (**1**-Cl), which was purified by recrystallization from CH_3OH/Et_2O. Single crystals of **1**-Cl that were suitable for crystallographic analysis were obtained from CH_3CN at −20 °C.[9]

The crystal structure of **1**-Cl (Figure 1) reveals a square-pyramidal ($\tau = 0.03$) iron center with an apical chloride ligand and the tetradentate L1 occupying the basal plane with metal–ligand distances that are typical of a high-spin iron(II) center.[6] The dioxoazabicyclic moiety, which serves as the framework to tether the pyridines and the bidentate carboxylate, wraps underneath the iron center and prevents the coordination of another ligand *trans* to the chloride. This ligand conformation appears energetically stable with the cyclohexyl ring in the chair conformation and the three methyl groups situated equatorially. This conformation positions the carboxylate to bind in a bidentate fashion to the iron center.

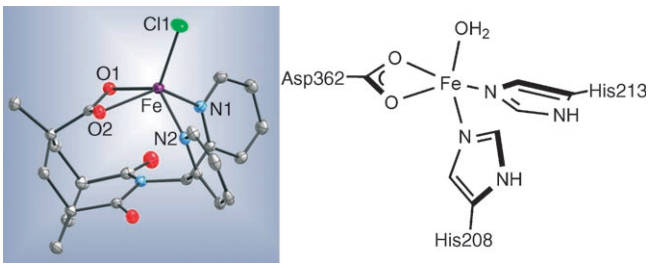

Figure 1. The ORTEP plot for $[Fe^{II}(L1)(Cl)]$ (**1**-Cl) showing 50% probability ellipsoids (left) and the mono-iron site of the substrate-bound form of naphthalene 1,2-dioxygenase (right, PDB 1O7G). Hydrogen atoms and noncoordinated solvent molecules have been omitted for clarity. Selected bond lengths are listed in Table 1.

Complex **1**-Cl differs in some respects from other iron(II) complexes that model the 2-His-1-carboxylate triad (**2**–**4**, Table 1).[6] Complexes **2**[6a,b] and **3**[6c] feature facial N,N,O ligand sets in which the carboxylate (or carboxamide) moiety is bound in a monodentate fashion, with Fe–O bond lengths (2.00–2.08 Å) that are shorter than for the bidentate carboxylate in **1**-Cl (2.15 Å). Furthermore, these are isolated as six-coordinate ML_2 complexes. On the other hand, **1**-Cl and **4**[6d] are both five-coordinate complexes with N_2O_2Cl ligand sets and resemble the iron centers found in the substrate-bound complexes of two Rieske dioxygenases (Figure 1 and Table 1). The metal–ligand distances found for **1**-Cl, however, more closely approximate those in the enzymes, particularly the more symmetric binding of the bidentate carboxylate. The main difference between **1**-Cl and the enzyme complexes lies in the arrangement of the ligands. For **1**-Cl, the chloride is the apical ligand, but for the enzymes, the water ligand that corresponds to the chloride occupies a nonapical position. Nevertheless, in either arrangement, there appears to be sufficient coordination flexibility to allow coordination of a bidentate oxidant in place of the chloride or water.

Table 1: Bond lengths [Å] and τ values observed for the iron centers in **1**–**4** and the substrate-bound forms of NDO and NBDO.

	1-Cl	**2** and **3**	**4**	NDO[a]	NBDO[b]
Fe-N1[c]	2.124(2)	2.15–2.35	2.226	2.0	2.1
Fe-N2[c]	2.137(2)	2.15–2.35	2.221	2.1	2.2
Fe-O1	2.145(1)	2.00–2.08	2.058	2.4	2.3
Fe-O2	2.150(1)	–	2.360	2.3	2.4
Fe-Cl/OH_2	2.250(1)		2.258	2.1	2.2
τ	0.03		0.49	0.51	0.20

[a] PDB 1O7G. [b] PDB 2BMQ. [c] For NDO, N1 = His 213 and N2 = His 208; for NBDO, N1 = His 211 and N2 = His 206.

To investigate whether **1**-Cl may serve also as a functional model of Rieske dioxygenases, reactions with H_2O_2 as the oxidant were carried out in the presence of olefin substrates. The results listed in Table 2 reveal that **1**-Cl can activate H_2O_2 to epoxidize electron-rich olefins. Epoxidation occurred with some loss of configuration for *cis*-2-heptene, with 47% retention of configuration (% RC; see also the footnote in Table 2) for *cis*-epoxide formation. However, only about a 30% yield of epoxide was obtained relative to iron complex.

The oxidation of electron-poor olefins, such as acrylate and fumarate, by **1**-Cl/H_2O_2 was even less effective, with only trace amounts of product observed in the reactions; instead, these oxidations afforded diols, the *cis*-diol in the case of fumarate. Our previous studies of other bio-inspired non-heme iron oxidation catalysts have demonstrated a requirement for *cis*-labile sites on the metal center to effect *cis*-

Table 2: Epoxidation (E) and *cis*-dihydroxylation (D) of olefins promoted by **1**-Cl and **1**-OTf with H_2O_2 oxidant.[a]

	1-Cl		**1**-OTf	
Substrate	E	D	E	D
cis-2-heptene	0.32(4) [47]	< 0.05	0.37(1) [51]	0.47(5) [96]
1-octene	0.26(6)	< 0.05	0.11(1)	0.67(2)
tert-butyl acrylate	< 0.05	0.08(1)		0.58(4)
dimethyl fumarate	< 0.05	< 0.05 [99]		0.42(4) [99]

[a] Reaction conditions: H_2O_2 (10 equiv per iron) was added by a syringe pump over a 25-min period to a solution of **1**-X (0.7 mM) and substrate (0.35 M) in CH_3CN under argon. Product yields were analyzed following 120 min of additional stirring. Yields are expressed as μmol product per μmol iron complex with standard deviation values shown in parentheses. Numbers in square brackets represent %RC values; $\%RC = 100 \times (A-B)/(A+B)$, where *A* is the yield of *cis*-diol or epoxide with retention of configuration and *B* is the yield of epimer.

dihydroxylation.[10] Thus, the small yields of diol may be due to partial loss of the chloride ligand during the reaction.

To test this hypothesis, pale yellow **1**-Cl was treated with a single equivalent of AgOTf (OTf = trifluoromethanesulfonate) in CH_3CN to precipitate AgCl and form a greenish-brown complex formulated as [Fe^{II}(L1)OTf] (**1**-OTf). Reaction of **1**-OTf with H_2O_2 in the presence of olefin substrates yielded epoxide and *cis*-diol products (Table 2). With 1-octene, the epoxide-to-diol ratio dramatically changed from > 50:1 for **1**-Cl in favor of epoxide to 1:6 for **1**-OTf in favor of diol; even electron-poor olefins could be oxidized to diols in comparable yield. Dihydroxylation occurs in a highly stereoselective fashion, with the diols from *cis*-2-heptene and dimethyl fumarate with %RC values of 96% and 99%, respectively. Like **1**-Cl, **1**-OTf affords less than one turnover of product, suggesting that the active oxidant cannot be regenerated, even in the presence of more H_2O_2 (see the Supporting Information). In support, the mass spectra of reaction solutions at the end of the reaction show evidence only for the free ligand, indicating the decomposition of the complex during the course of the reaction (see the Supporting Information).

^{18}O-labeling experiments have proven instructive in deducing mechanisms by establishing the source of the oxygen atoms incorporated into the products.[6c,10,11] For **1**-Cl, the required addition of 200 equivalents of H_2O (present in the 10 wt% $H_2{}^{18}O_2$ solution) significantly inhibited epoxide formation. As a result, labeling experiments were carried out with a 1:3 mixture of $H_2{}^{18}O_2/H_2{}^{16}O_2$ to decrease the amount of added water (75 equiv H_2O). A 20% incorporation of ^{18}O was observed for the *cis*-2-heptene oxide product (80% normalized), whereas the corresponding experiment with 75 equivalents of added $H_2{}^{18}O$ afforded only 3% label incorporation (Table 3). Thus, the *cis*-epoxide oxygen atom is derived mainly from H_2O_2. On the other hand, no label incorporation from either $H_2{}^{18}O$ or $H_2{}^{18}O_2$ was observed for the minor *trans*-epoxide product, suggesting that this product derives from autoxidation.

For **1**-OTf, ^{18}O-labeling studies of the epoxidation of *cis*-2-heptene showed nearly identical results as those for **1**-Cl. On the other hand, dihydroxylation of *cis*-2-heptene and 1-octene yielded diols with 85% and 81% double label incorporation, respectively. Furthermore with 50:50 $H_2{}^{16}O_2/H_2{}^{18}O_2$, the two diol oxygens incorporated were derived from one molecule of H_2O_2, demonstrating that **1**-OTf serves as an exemplary dioxygenase model. Interestingly, the complementary $H_2{}^{18}O$ labeling experiment revealed 7–8% singly labeled *cis*-diol products.

The reactivities of **1**-Cl and **1**-OTf suggest the formation of distinct oxidants for epoxidation and dihydroxylation (Scheme 2). Given the comparable epoxide yields and ^{18}O-labeling results, both **1**-Cl/H_2O_2 and **1**-OTf/H_2O_2 likely produce a common oxidant that epoxidizes *cis*-2-heptene by oxygen-atom transfer from bound H_2O_2. A plausible epoxidizing agent, the η^2-OOH species shown in Scheme 2 is analogous to that observed for the ESO_2 adduct of NDO and is proposed for non-water-assisted epoxidation by Fe(bpmen) (bpmen = *N*,*N*′-dimethyl-*N*,*N*′-bis(2-pyridylmethyl)-1,2-diaminoethane).[12] More importantly, a dihydroxylating agent must be generated that incorporates both oxygen atoms of H_2O_2 into the *cis*-diol product and is capable of some label exchange with H_2O. We propose that this oxidant is formed upon dissociation of X (much more favored for OTf than for Cl) that promotes the isomerization of the Fe-η^2-OOH unit to a higher-valent iron-oxo/hydroxo species. Binding of H_2O to the iron center during oxidation provides a mechanism for label exchange, like that shown previously for **3**.[6c] We note that NDO also exhibits label exchange with solvent water in the dihydroxylation of naphthalene by H_2O_2 (Table 3),[13] implicating involvement of

Table 3: Results of ^{18}O-labeling experiments.[a]

	Substrate	Product(s)	$H_2{}^{18}O_2$[b]	$H_2{}^{18}O$[b]
1-Cl	*cis*-2-heptene	*cis*-oxide	20/80	97/3
		trans-oxide	100/0	100/0
1-OTf	*cis*-2-heptene	*cis*-oxide	23/77	99/1
		trans-oxide	98/2	100/0
		cis-diol	1/14/85	93/7
	1-octene	*cis*-diol	1/18/81	92/8
NDO[c]	naphthalene	*cis*-dihydrodiol	1/10/89	96/3

[a] For reaction conditions, see footnote [a] of Table 2. [b] Values are reported as the percentage of 0/1 O label that is incorporated into epoxide products and 0/1/2 O labels incorporated into diol products. [c] Results reported in Ref. [13].

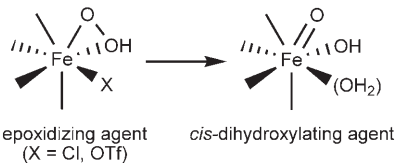

Scheme 2. Proposed active oxidants derived from **1**-X with H_2O_2.

an analogous dihydroxylating agent in the enzyme mechanism.

We have thus designed a ligand that gives rise to iron complexes that approximate the 2-His-1-carboxylate environment of the Rieske dioxygenases. Even though less than one turnover of olefin oxidation is achieved, the activation of H_2O_2 by the triflate complex leads to the *cis*-dihydroxylation of double bonds. Label incorporation from $H_2{}^{18}O$ implicates a high-valent iron-oxo species as the oxidant for this novel reaction.

Experimental Section

HL1: A mixture of Kemp's acid chloroanhydride[7] (970 mg, 3.75 mmol), di-(2-pyridyl)methylamine[8] (842.8 mg, 2.86 mmol), and DMAP (4-dimethylaminopyridine, 37 mg) in freshly distilled pyridine (12 mL) was heated under argon to 90 °C and stirred for 2 days. Upon cooling to room temperature, the solvent was removed in vacuo, leaving a dark solid. Water (10 mL) was added to this solid, and the product was extracted into ethyl acetate (3×25 mL). This crude yellow product obtained from the extraction was purified with chromatography on a silica gel column with an ethyl acetate/methanol gradient to obtain a white solid (1.35 g, 89 % yield), which was characterized by ^{1}H and ^{13}C NMR spectroscopy (see the Supporting Information). Minor impurities included monoacylated and acyclic diacylated products. ESIMS (CH_3CN): *m*/*z* 408 ($[HL1+H]^+$).

1-Cl: A solution of HL1 (168.9 mg, 0.44 mmol) and Et_3N (41.9 mg, 0.44 mmol) in CH_3CN (2 mL) was added dropwise to a stirred solution of $FeCl_2$ (52.6 mg, 0.44 mmol) in CH_3CN (2 mL) in an anaerobic glove box. Overnight stirring at room temperature afforded a yellow solid, which was recrystallized from MeOH/Et_2O (112 mg, 51 % yield). Further recrystallization in CH_3CN at −20 °C resulted in the overnight formation of yellow blocks suitable for X-ray crystallographic studies. UV/Vis (CH_3CN), λ_{max} (ε [$M^{-1}cm^{-1}$]): 264 (5800), 310 (1600), 450 nm onset. ESIMS (CH_3OH): *m*/*z* 869 ($[Fe(L1)_2+H]^+$), 498 ($[Fe(L1)(Cl)+H]^+$), 462 ($[Fe(L1)]^+$), 408 ($[HL1+H]^+$). Elemental analysis (%) calcd for $C_{23}H_{24}ClFeN_3O_4$: C 55.50, H 4.86, N 8.44, Cl 7.12; found: C 55.68, H 5.14, N 8.76, Cl 6.87.

1-OTf: Ag(OTf) (67.8 mg, 0.264 mmol) in CH_3CN (1.5 mL) was added to a yellow suspension of **1**-Cl (131.2 mg, 0.264 mmol) in CH_3CN (2.5 mL) in an anaerobic glove box. After stirring at room temperature overnight, the reaction suspension was concentrated to produce a brown-green dark solid. UV/Vis (CH_3CN), λ_{max} (ε [$M^{-1}cm^{-1}$]): 260 (9100), 356 nm (sh, 3000). ESIMS (CH_3OH; see Figure S4 in the Supporting Information): *m*/*z* 869 ($[Fe(L1)_2+H]^+$), 612 ($[Fe(L1)(OTf)+H]^+$), 462 ($[Fe(L1)]^+$), 408 ($[HL1+H]^+$).

Received: August 25, 2006
Revised: October 2, 2006
Published online: November 10, 2006

Keywords: dihydroxylation · dioxygenases · enzyme models · epoxidation · oxidation

[1] *Biological Inorganic Chemistry* (Eds.: I. Bertini, H. B. Gray, E. I. Stiefel, J. S. Valentine), University Science Books, Sausalito, **2006**.
[2] a) M. Costas, M. P. Mehn, M. P. Jensen, L. Que, Jr., *Chem. Rev.* **2004**, *104*, 939; b) M. M. Abu-Omar, A. Loaiza, N. Hontzeas, *Chem. Rev.* **2005**, *105*, 2227; c) K. D. Koehntop, J. P. Emerson, L. Que, Jr., *J. Biol. Inorg. Chem.* **2005**, *10*, 87.
[3] A. Karlsson, J. V. Parales, R. E. Parales, D. T. Gibson, H. Eklund, S. Ramaswamy, *Science* **2003**, *299*, 1039.
[4] R. Friemann, M. M. Ivkovic-Jensen, D. J. Lessner, C.-L. Yu, D. T. Gibson, R. E. Parales, H. Eklund, S. Ramaswamy, *J. Mol. Biol.* **2005**, *348*, 1139.
[5] a) D. T. Gibson, V. Subramanian, in *Microbial Degradation of Organic Compounds* (Ed.: D. T. Gibson), Marcel Dekker, New York, **1984**, p. 181; b) L. P. Wackett, *Enzyme Microb. Technol.* **2002**, *31*, 577; c) D. J. Ferraro, L. Gakhar, S. Ramaswamy, *Biochem. Biophys. Res. Commun.* **2005**, *338*, 175.
[6] a) A. Beck, B. Weibert, N. Burzlaff, *Eur. J. Inorg. Chem.* **2001**, 521; b) A. Beck, A. Barth, E. Hubner, N. Burzlaff, *Inorg. Chem.* **2003**, *42*, 7182; c) P. D. Oldenburg, A. A. Shteinman, L. Que, Jr., *J. Am. Chem. Soc.* **2005**, *127*, 15672; d) S. J. Friese, B. E. Kucera, L. Que, Jr., W. B. Tolman, *Inorg. Chem.* **2006**, **45**, 8003.
[7] D. S. Kemp, K. S. Petrakis, *J. Org. Chem.* **1981**, *46*, 5140.
[8] M. Renz, C. Hemmert, B. Meunier, *Eur. J. Org. Chem.* **1998**, 1271.
[9] Single-crystal structure and refinement data for **1**-Cl: $C_{23}H_{24}ClFeN_3O_4$, $M_w = 497.75$, monoclinic, space group $P2_1/n$, $a = 10.8970(6)$, $b = 13.3325(7)$, $c = 15.0564(8)$ Å, $\alpha = 90.000(1)$, $\beta = 95.9000(1)$, $\gamma = 90.000(1)°$, $V = 2175.9(2)$ Å^3, $Z = 4$, $\rho_{calcd} = 1.519$ Mg m^{-3}, $Mo_{K\alpha}$ radiation ($\lambda = 0.71073$ Å, $\mu = 0.852$ mm^{-1}), $T = 173(2)$ K. A total of 4946 ($R_{int} = 0.0388$) independent reflections with $2\theta < 27.49°$ were collected. The resulting parameters were refined to converge at $R_1 = 0.0379$ ($I > 2\theta$) for 292 parameters on 4946 independent reflections ($wR_2 = 0.0926$). Max./min. residual electron density 0.501/−0.281 e Å^{-3}; GOF = 1.006. Further experimental details are provided in the Supporting Information. CCDC-613027 contains the supplementary crystallographic data for this paper. These data can be obtained free of charge from The Cambridge Crystallographic Data Centre via www.ccdc.cam.ac.uk/data_request/cif.
[10] a) K. Chen, M. Costas, J. Kim, A. K. Tipton, L. Que, Jr., *J. Am. Chem. Soc.* **2002**, *124*, 3026; b) K. Chen, M. Costas, L. Que, Jr., *Dalton Trans.* **2002**, 672.
[11] a) K. Chen, L. Que, Jr., *Angew. Chem.* **1999**, *111*, 2365; *Angew. Chem. Int. Ed.* **1999**, *38*, 2227; b) K. Chen, L. Que, Jr., *J. Am. Chem. Soc.* **2001**, *123*, 6327; c) M. Klopstra, G. Roelfes, R. Hage, R. M. Kellogg, B. L. Feringa, *Eur. J. Inorg. Chem.* **2004**, 846.
[12] D. Quiñonero, K. Morokuma, D. G. Musaev, R. Mas-Ballesté, L. Que, Jr., *J. Am. Chem. Soc.* **2005**, *127*, 6548.
[13] M. D. Wolfe, J. D. Lipscomb, *J. Biol. Chem.* **2003**, *278*, 829.

